purified using standard proteinase K digestion and phenol/chloroform extraction methods.

2.2. Differential polymerase chain reaction assay for *PTEN*

The differential polymerase chain reaction (PCR) method for the homozygous deletion of *PTEN* was based on a modification of a reported method using GAPDH as the internal control [8]. Although 9 exons are known to code for the *PTEN* gene, *PTEN* mutations and deletions are reported to be relatively rare in the region from exon 1 to 4 [6,7]; therefore, we evaluated the deletion status of the *PTEN* gene in the region extending from exon 5 to 9. Samples of DNA were added to a PCR mix with a total volume of 25 μL containing 10 mmol/L Tris-HCl (pH 8.3), 1.5 mmol/L $MgCl_2$, 0.25 mmol/L dNTP, 0.5 U Taq DNA polymerase, 1.0 μmol/L of each of the *PTEN* primers, and 1.0 μmol/L of each of the GAPDH primers. The sequences of the primers used were those of previously described pairs of primers [6,21]. Polymerase chain reaction was carried out in a Gene Amp PCR System 9600 (Perkin Elmer, Foster City, Calif) for 30 cycles after the first denaturation at 96°C for 5 minutes (96°C for 1 minute, 58°C for 1 minute, 72°C for 1 minute). After amplification, 10 μL of PCR products were electrophoresed through 8.0% acrylamide gel, and the intensities of the DNA products were quantified using National Institutes of Health Imaging software ver. 1.56. Values of less than 30% for the target gene/internal control ratio were considered to represent homozygous deletion [8,22].

2.3. Bisulfite modification and methylation-specific PCR

Bisulfite modification was performed using a DNA modification kit (Intergen, Purchase, NY) according to the manufacturer's protocol. The modified DNA was used for the methylation-specific PCR. The sequences of the primers and the primer conditions used were previously described [10]. Polymerase chain reaction was carried out for 35 cycles after the first denaturation at 95°C for 15 minutes (94°C for 30 seconds, 60°C for 1 minute, 72°C for 1 minute); then, a final 5-minute extension was carried out at 72°C. Each of the PCR products (10 μL) was directly loaded onto 2% agarose gel, stained with ethidium bromide, and directly visualized under UV illumination.

2.3.1. Immunohistochemistry

Immunohistochemical analysis was performed using mouse immunoglobulin G monoclonal antibodies against PTEN (1:200, AG Science, San Diego, Calif) and Ki-67 (MIB-1; 1:100, Immunotech, Marseille, France). Four-micrometer-thick histologic sections were cut, mounted on glass slides coated by 3-aminopropyltriethoxysilane, and the slides were air-dried overnight at room temperature. The sections were deparaffinized in xylene and dehydrated in ethanol. After dehydration, the endogenous peroxidase was blocked by methanol containing 3% H_2O_2 for 30 minutes. For staining with the above antibody, specimens were pretreated with citrate buffer (0.01 mol/L citric acid: pH 6.0) 4 times, each for 5 minutes at 100°C in a microwave oven. The sections were incubated with the primary antibody at 4°C overnight, followed by staining with a streptavidin-biotin-peroxidase kit (Nichirei, Tokyo, Japan). The sections were then finally reacted in a 3,3′-diaminobenzidine, peroxytrichloride substrate solution, counterstained with hematoxylin, and then mounted. The evaluation of immunohistochemical staining for PTEN was based on a modification of a previously reported method [23]. The extent of staining was graded as follows: 0, staining was observed in less than 1% of the tumor cells; 1, staining in 1% to 10% of the tumor cells; 2, staining in 10% to 50% of the tumor cells; and 3, staining in >50% of the tumor cells. The overall intensity of the staining was also assessed as follows: 0, no staining; 1, weak staining; 2, moderate staining; and 3, strong staining. The final score (range, 0-9) was obtained by multiplying the extent of staining with the intensity. When the final score was less than 4, the sample was considered as reflective of decreased expression. When the tumor cells failed to stain in all areas or when they were stained in only some of those areas, we confirmed the staining of admixed nonneoplastic cells or mesenchymal tissues (normal smooth muscle and nerve sheath tissues) as a positive control. The MIB-1 labeling index (MIB-1-LI) was determined as the percentage of positive cells by counting the positively stained nuclei in at least 1000 tumor cells.

2.3.2. Statistical analysis

Fisher exact test or Mann-Whitney *U* test was used to evaluate the association between 2 dichotomous variables. A *P* value of less than .05 was considered to indicate statistical significance.

3. Results

3.1. Clinical and histologic findings

The clinicopathologic data are summarized in Table 1. The age of the patients ranged from 1 to 93 years (average, 59.8 years). Twenty-four patients were male and 24 were female.

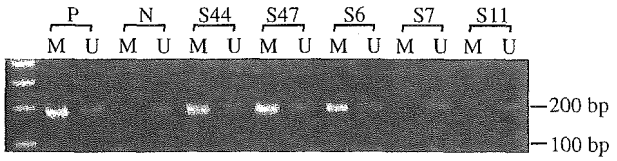

Fig. 1 Methylation-specific PCR analysis of *PTEN*. PCR products amplified by unmethylated (U) and methylated (M) specific primers. Cases S44 (MPNST), S47 (MPNST), and S6 (MPNST) showed hypermethylation of the *PTEN* gene promoter. P indicates positive control; N, negative control.

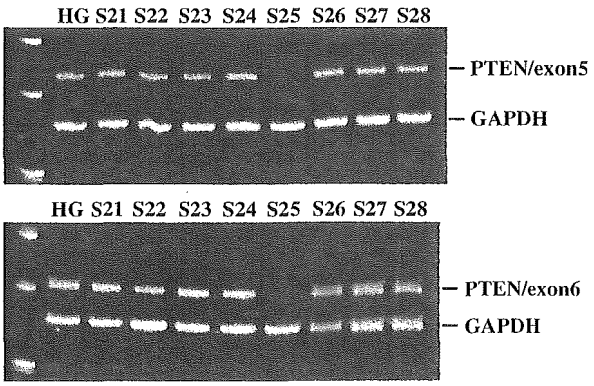

Fig. 2 Differential PCR for PTEN homozygous deletion. Case S25 (MFH) displayed very low levels (<30% ratio) of the PCR products of the *PTEN* gene.

Twenty-five patients were affected in a lower extremity, 8 in an upper extremity, 6 in the buttock, 5 in the retroperitoneum, and 1 each in the shoulder, posterior mediastinum, inferior vena cava, and spinal cord. Tumor size was available for all cases and ranged from 2 to 26 cm (average, 8.5 cm). Forty cases were primary tumors and 8 were recurrent tumors. The FNCLCC grading and AJCC stage were available in 40 cases. In the FNCLCC grading system, 12 were considered to be grade 2 and 26 were grade 3. With regard to AJCC stage, 1 case was considered to be stage I, 20 cases were stage II, 16 were stage III, and 1 was stage IV.

3.2. Promoter hypermethylation of *PTEN*

First, we examined methylation status in 48 STSs cases that we had previously examined for *PTEN* mutation [19]. Promoter hypermethylation of the *PTEN* gene was detected in 6 (13%) of 48 STS cases (Fig. 1). In all cases with promoter hypermethylation, both unmethylated as well as methylated signals were observed. Of 6 cases with promoter hypermethylation, 5 were MPNST, and the remaining case was MFH (storiform pleomorphic type). There was no statistically significant correlation between *PTEN* methylation and the clinicopathologic parameters (data not shown).

3.3. Homozygous deletion

Homozygous deletion of the *PTEN* gene was detected in 1 (2%) of the 48 STS cases examined (Fig. 2). The histologic type of 1 case with homozygous deletion was MFH. In total, *PTEN* gene alteration was observed in 9 (19%) of 48 STS cases (promoter methylation, 6 cases; mutation, 2 cases; homozygous deletion, 1 case) (Table 2).

3.4. Immunohistochemical analysis of PTEN protein

To evaluate the nature of *PTEN* alteration associated with a decrease in PTEN expression, we examined the expression of PTEN using immunohistochemical analysis. Paraffin-embedded tissues were available for immunohistochemical analysis in 38 cases, including 9 cases with *PTEN* gene alteration and 29 cases without gene alteration. Eleven (29%) of the 38 STS cases revealed decreased expression of PTEN protein (Fig. 3). Three cases with *PTEN* gene alteration showed decreased expression of PTEN protein; 2 of these cases showed promoter methylation and 1 case showed homozygous deletion. *PTEN* gene alteration was not significantly correlated with the decreased expression of PTEN protein. No statistically significant correlation between PTEN expression and the clinicopathologic parameters was identified (data not shown). MIB-1 labeling index ranged from 5.2 to 39.8 (mean: 18.1) in our series. Decreased PTEN expression was significantly correlated with high MIB-1-LI in the 38 STS cases examined ($P = .0441$) (Table 3).

4. Discussion

The *PTEN* gene was identified as a tumor suppressor gene located on chromosome 10q23.3, and encodes a cytoplasmic protein that controls cellular processes, such as cell cycling and apoptosis, as a regulator of phosphatidylinositol 3-kinase [24]. A decrease or loss of PTEN expression has been described in many types of carcinomas

Table 2 *PTEN* alteration in STSs

Case	Sex	Age	Diagnosis	Location	Size (cm)	PTEN expression	*PTEN* alteration
S1	M	42	MFH	Lower extremity	9	N	Methylation
S6	F	27	MPNST	Buttock	15	N	Methylation
S15	F	67	MPNST	Lower extremity	6	N	Methylation
S21	M	47	MPNST	Lower extremity	15	N	Methylation
S22	F	43	LMS	Inferior vena cava	3	N	Mutation[a]
S23	M	55	LMS	Retroperitoneum	26	N	Mutation[a]
S25	F	83	MFH	Upper extremity	5	D	HD
S44	M	76	MPNST	Lower extremity	5	D	Methylation
S47	F	4	MPNST	Retroperitoneum	7	D	Methylation

N indicates normal expression; D, decreased expression; HD, homozygous deletion.

[a] The results of *PTEN* gene mutation have been previously reported [19].

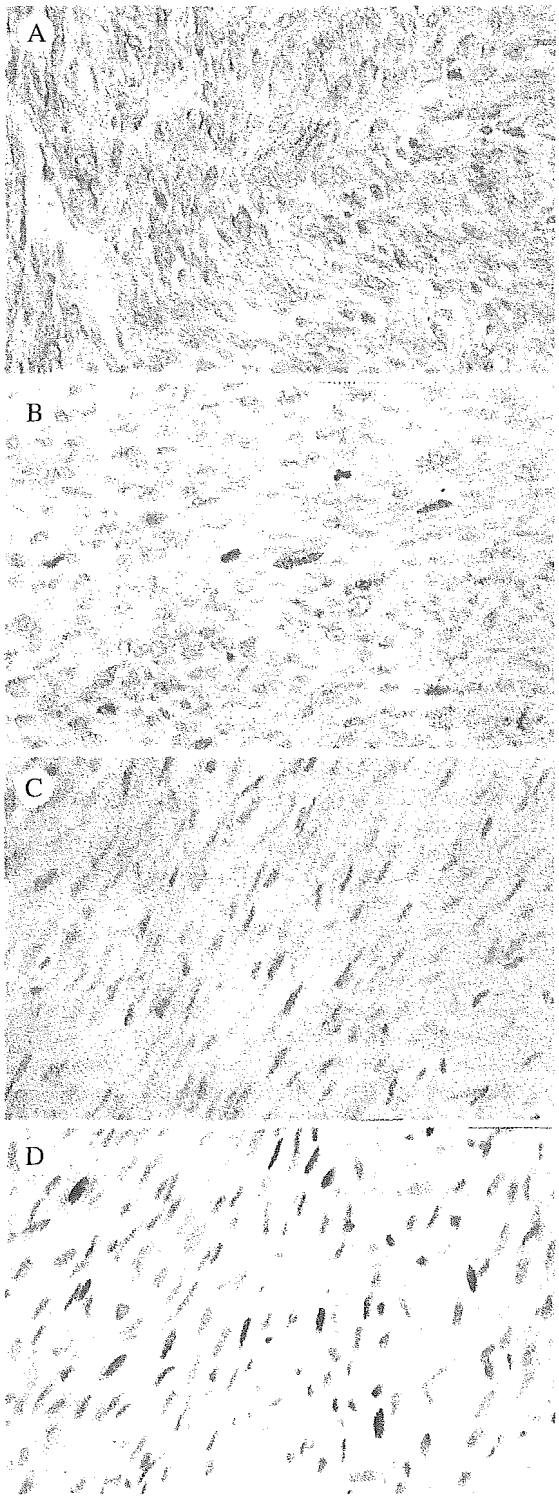

Fig. 3 Immunohistochemical staining of PTEN in STSs. A, Immunohistochemistry showing cytoplasmic staining in the majority of tumor cells (MFH, case S3). This case had no alteration of the *PTEN* gene. B, Immunohistochemistry of MIB-1 in case S3. MIB-1-LI was 12.2. C, A loss of PTEN expression was observed in the majority of the tumor cells, but the surrounding normal tissue showed strong cytoplasmic positivity. This case showed hypermethylation of the *PTEN* gene (MPNST, case S44). D, Immunohistochemistry of MIB-1 in case S44. MIB-1-LI was 27.6.

Table 3 Correlation between PTEN immunoreactivity and MIB-1-LI (n = 38)

	MIB-1-LI (mean ± SD)	
PTEN expression		
Normal	16.0 ± 8.5	P = .0441[a]
Decreased	23.2 ± 10.1	

Mann-Whitney U test.
[a] Statistically significant.

and other malignancies [25-27]. In a previous study of mesenchymal tumors, 4 (33%) of 12 MPNST cases showed decreased expression of PTEN protein [28]. The present immunohistochemical analysis of 38 STS cases revealed that the rate of PTEN inactivation at the protein level is relatively rare (29%). Loss of PTEN expression has been associated with advanced stage and metastasis in some types of malignancy [25,26,29]. Furthermore, Halvorsen et al [30] demonstrated that concomitant loss of PTEN and p27 expression was strongly associated with cell proliferation by Ki-67 in prostate cancer. In this study, there was a statistically significant correlation between decreased PTEN expression and cell proliferation induced by Ki-67 in 38 STSs, indicating that PTEN expression may be a useful indicator of tumor cell proliferation in these tumors; however, analysis of a larger number of cases will be necessary to clarify the potential role of PTEN in this context.

The following primary mechanisms of inactivation of the *PTEN* gene have been proposed: homozygous deletion, mutation, and promoter hypermethylation. Although mutations of the *PTEN* gene have frequently been detected in certain malignancies, we previously reported that mutations of this gene were rare (2%) in a series of 51 STSs cases [19]; similar low frequencies have been reported among cases of chondrosarcoma [31]. Homozygous deletion of the *PTEN* gene has been demonstrated in various types of malignancy, and such deletion is known to play an important role in inactivation [9]. Loss of heterozygosity of chromosome 10q has been described in bone and STSs [14-18]. In the present study, homozygous deletion of the *PTEN* gene was detected only in 1 (2%) of 48 cases by differential PCR. One case of homozygous deletion showed decreased expression of PTEN protein; in contrast, 2 cases of mutation revealed normal expression of PTEN protein. According to the 2-hit hypothesis of Knudson [32], *PTEN* mutation might have occurred in only 1 allele in the 2 cases of mutation. Those results, taken together with the present findings, indicate that homozygous deletion, as well as *PTEN* mutation, are rare events associated with *PTEN* inactivation in STSs.

Promoter methylation is a representative example of the transcriptional silencing of tumor suppressor genes. Methylation of the CpG island of *PTEN* has been described in various types of malignancy, and gene silencing by promoter methylation of the *PTEN* gene has been also demonstrated [10-13]. In the present study, *PTEN* methyl-

ation was recognized in 6 (13%) of 48 STS cases by methylation-specific PCR. Our methylation analysis revealed decreased expression of PTEN protein in only 2 (33%) of 6 cases of *PTEN* methylation, indicating that the inactivation of the *PTEN* gene may be partially accounted for by promoter methylation of this gene in STSs. A total of 9 (19%) of 48 STS cases showed *PTEN* alteration, and the inactivation of *PTEN* was recognized in only 3 (33%) of 9 cases with *PTEN* alteration. Taking these findings into consideration, genetic and epigenetic alterations of *PTEN*, such as homozygous deletion, mutation, and promoter methylation, may be less associated with the inactivation of this gene. However, we also demonstrated that the rate of PTEN inactivation at the protein level was more frequent than that identified at the genetic level, which was recognized in 29% of the STS cases considered here. Furthermore, these results indicated that the loss of protein detected by immunohistochemistry might reflect a majority of possible mechanisms resulting in PTEN inactivation; such putative mechanisms include indirect inactivation, such as a loss of *PTEN*-directed transcription factor, and various posttranscriptional modifications.

Our results demonstrated that 5 of 6 cases with *PTEN* methylation were cases of MPNST. Previous cytogenetic studies have revealed that the loss of chromosome 10q is quite rare in cases of MPNST [33]. In addition, *PTEN* mutation was not observed in 12 MPNST cases [27], as was also found in our previous report [19]. With regard to alteration of the *PTEN* gene, epigenetic abnormalities, particularly promoter methylation, are suspected as playing an important role in the pathogenesis of MPNST, although further detailed analysis is still necessary.

In conclusion, *PTEN* gene alterations were recognized in 9 of 48 STS cases. Promoter methylation and homozygous deletion of the *PTEN* gene were both found to be relatively rare events associated with this tumor type, as is mutation of the gene itself. In addition, a decrease in PTEN expression was recognized in only 3 (33%) of 9 cases with *PTEN* alteration. These results suggest that *PTEN* gene alterations play a minor role in the inactivation of *PTEN* in STSs. Furthermore, although further detailed analysis remains necessary, PTEN expression may be the dominant factor of tumor cell proliferation in STS cases.

Acknowledgments

We are grateful to Y Nouzuka and N Tateishi for their excellent technical assistance.

References

[1] Di Cristofano AD, Pandolfi PP. The multiple roles of *PTEN* in tumor suppression. Cell 2000;100:387-90.

[2] Rhei E, Kang L, Bogomolniy F, et al. Mutation analysis of the putative tumor suppressor gene *PTEN/MMAC1* in primary breast carcinomas. Cancer Res 1997;57:3657-9.

[3] Risinger JI, Hayes K, Maxwell GL, et al. *PTEN* mutation in endometrial cancers is associated with favorable clinical and pathologic characteristics. Clin Cancer Res 1998;4:3005-10.

[4] Tashiro H, Blazes MS, Wu R, et al. Mutations in *PTEN* are frequent in endometrial carcinoma but rare on other common gynecological malignancies. Cancer Res 1997;57:3935-40.

[5] Yokomizo A, Tindall DJ, Hartmann L, et al. Mutation analysis of the putative tumor suppressor *PTEN/MMAC1* in human ovarian cancer. Int J Oncol 1998;13:101-5.

[6] Minaguchi T, Yoshikawa H, Oda K, et al. *PTEN* mutation located only outside exons 5, 6, and 7 is an independent predictor of favorable survival in endometrial carcinomas. Clin Cancer Res 2001; 7:2636-42.

[7] Ali IU, Schriml LM, Dean M. Mutation spectra of *PTEN/MMAC1* gene: a tumor suppressor with lipid phosphatase activity. J Natl Cancer Inst 1999;91:1922-32.

[8] Chen C, Samaranayake LP, Zhou H, et al. Homozygous deletion of *PTEN* tumor-suppressor gene is not a feature in oral squamous cell carcinoma. Oral Oncol 2000;36:95-9.

[9] Wang SI, Parsons R, Ittmann M. Homozygous deletion of the *PTEN* tumor suppressor gene in a subset of prostate adenocarcinomas. Clin Cancer Res 1998;4:811-5.

[10] Soria JC, Lee HY, Lee JI, et al. Lack of *PTEN* expression in non-small cell lung cancer could be related to promoter methylation. Clin Cancer Res 2002;8:1178-84.

[11] Sato K, Tamura G, Tsuchiya T, et al. Analysis of genetic and epigenetic alterations of the *PTEN* gene in gastric cancer. Virchows Arch 2002;440:160-5.

[12] Kang YH, Lee HS, Kim WH. Promoter methylation and silencing of *PTEN* in gastric carcinoma. Lab Invest 2002;3:285-91.

[13] Salvesen HB, MacDonald N, Ryan A, et al. *PTEN* methylation is associated with advanced stage and microsatellite instability in endometrial carcinoma. Int J Cancer 2001;91:22-6.

[14] El-Rifai W, Sarlomo-Rikala M, Knuutila S, et al. DNA copy number change in development and progression in leiomyosarcoma of soft tissue. Am J Pathol 1998;153:985-90.

[15] Otano-Joos M, Mechtersheimer G, Ohl S, et al. Detection of chromosomal imbalances in leiomyosarcoma by comparative genomic hybridization and interphase cytogenetics. Cytogenet Cell Genet 2000;90:86-92.

[16] Mandahl N, Fletcher CDM, Dal Cin P, et al. Comparative cytogenetic study of spindle cell and pleomorphic leiomyosarcomas of soft tissues: a report from the CHAMP study group. Cancer Genet Cytogenet 2000;116:66-73.

[17] Derre J, Lagace R, Nicolas A, et al. Leiomyosarcomas and most malignant fibrous histiocytomas share very similar comparative genomic hybridization imbalances: an analysis of a series of 27 leiomyosarcomas. Lab Invest 2001;81:211-5.

[18] Raskind WH, Conrad EU, Matsushita M. Frequent loss of heterozygosity for markers on chromosome arm 10q in chondrosarcomas. Genes Chromosomes Cancer 1996;16:138-43.

[19] Saito T, Oda Y, Kawaguchi K, et al. *PTEN/MMAC1* gene is a rare event in soft tissue sarcomas without specific balanced translocations. Int J Cancer 2003;104:175-8.

[20] Coindre JM, Bui NB, Bonichon F, et al. Histopathologic grading in spindle cell soft tissue sarcomas. Cancer 1998;61: 2305-9.

[21] Liu J, Babaian DC, Liebert M, et al. Inactivation of MMAC1 in bladder transitional-cell carcinoma cell lines and specimens. Mol Carcinog 2000;29:143-50.

[22] Bostrom J, Cobbers JMJL, Wolter M, et al. Mutations of the *PTEN (MMAC1)* tumor suppressor gene in a subset of glioblastomas but not in meningiomas with loss of chromosome arm 10q1. Cancer Res 1998;58:29-33.

[23] Salvesen HB, Stefansson I, Kalvenes MB, et al. Loss of PTEN expression is associated with metastatic disease in patients with endometrial carcinoma. Cancer 2002;94:2185-91.

[24] Dahia PLM. *PTEN*, a unique tumor suppressor gene. Endocr Relat Cancer 2000;7:115-29.

[25] Whang YE, Wu X, Suzuki H, et al. Inactivation of the tumor suppressor *PTEN/MMAC1* in advanced human prostate cancer through loss of expression. Proc Natl Acad Sci U S A 1998;95: 5246-50.

[26] Rasheed BK, Stenzel TT, McLendon RE, et al. *PTEN* gene mutations are seen in high-grade but not in low-grade gliomas. Cancer Res 1997;57:4187-90.

[27] Risingner JI, Hayes K, Maxwell GL, et al. *PTEN* mutation on endometrial cancers is associated with favorable clinical and pathologic characteristics. Clin Cancer Res 1998;4:3005-10.

[28] Mawrin C, Kirches E, Boltze C, et al. Immunohistochemical and molecular analysis of p53, Rb, and PTEN in malignant peripheral nerve sheath tumors. Virchows Arch 2002;440:610-5.

[29] Hu T-H, Huang C-C, Lin P-R, et al. Expression and prognostic role of tumor suppressor gene *PTEN/MMAC1/TEP1* in hepatocellular carcinoma. Cancer 2003;97:1929-40.

[30] Halvorsen OJ, Haukaas SA, Akslen LA. Combined loss of PTEN and p27 expression is associated with tumor cell proliferation by Ki-67 and increased risk of recurrent disease in localized prostate cancer. Clin Cancer Res 2003;9:1474-9.

[31] Lin C, Meitner PA, Terek RM. *PTEN* mutation is rare in chondrosarcoma. Diagn Mol Pathol 2002;11:22-6.

[32] Knudson Jr AG, Hethcote HW, Brown BW. Mutation and childhood cancer: a probabilistic model for the incidence of retinoblastoma. Proc Natl Acad Sci U S A 1975;72:5116-20.

[33] Plaat BE, Molenaar WM, Mastik MF, et al. Computer-assisted cytogenetic analysis of 51 malignant peripheral-nerve-sheath tumors: Sporadic vs. neurofibromatosis-type-1-associated malignant schwannomas. Int J Cancer 1999;83:171-8.

ELSEVIER

Cancer Genetics and Cytogenetics 165 (2006) 98–105

CANCER GENETICS AND CYTOGENETICS

Chromosomal aberrations and microsatellite instability of malignant peripheral nerve sheath tumors: a study of 10 tumors from nine patients

Chikashi Kobayashi[a], Yoshinao Oda[a,*], Tomonari Takahira[a], Teiyu Izumi[a], Kenichi Kawaguchi[a], Hidetaka Yamamoto[a], Sadafumi Tamiya[a], Tomomi Yamada[b], Shinya Oda[c], Kazuhiro Tanaka[d], Shuichi Matsuda[d], Yukihide Iwamoto[d], Masazumi Tsuneyoshi[a,1]

[a]*Department of Anatomic Pathology, Graduate School of Medical Sciences, Kyushu University, 3-1-1 Maidashi, Higashi-ku, Fukuoka 812-8582, Japan*
[b]*Department of Medical Information Science, Graduate School of Medical Sciences, Kyushu University, Fukuoka, Japan*
[c]*National Kyushu Cancer Center, Fukuoka, Japan*
[d]*Department of Orthopedic Surgery, Graduate School of Medical Sciences, Kyushu University, Fukuoka, Japan*

Received 24 May 2005; received in revised form 1 July 2005; accepted 6 July 2005

Abstract Malignant peripheral nerve sheath tumor (MPNST) is an uncommon soft tissue neoplasm with a poor prognosis, occurring sporadically or associated with neurofibromatosis type 1 (NF1); however, the histogenesis of MPNST remains unclear, especially in sporadic tumors. There are two major forms of genomic instability in human cancer: chromosomal instability (CIN) and microsatellite instability (MSI). An inverse relationship has recently been demonstrated between CIN and MSI in colorectal cancers. CIN and MSI are suggested to be individual pathways, which are involved in the pathogenesis and which may lead to specific clinical and pathological characteristics. To elucidate the chromosomal aberration as a consequence of CIN and MSI status of MPNST, we karyotyped 10 MPNSTs from nine patients, and examined the MSI of seven microsatellite markers using high-resolution fluorescence microsatellite analysis; 2 out of 10 cases (20%) had normal karyotypes, and 8 out of 10 cases (80%) revealed structural and numerical chromosomal aberrations. Three of the 10 cases (30%) showed near triploidy. The most frequent aberration was −22 (40%), followed by +2, +14, −13, −17, and −18 (30% each). An MSI-low status was observed in 30% of cases; the remaining cases showed microsatellite stability. These findings suggest that chromosomal aberration as a consequence of CIN has a greater role in the pathogenesis of MPNST than does that due to MSI.

1. Introduction

Malignant peripheral nerve sheath tumor (MPNST) is an uncommon soft tissue neoplasm with a poor prognosis [1]. These tumors typically occur as sporadic tumors or in association with neurofibromatosis type 1 (von Recklinghausen disease; NF1). In NF1 patients, MPNSTs arise from a preexisting benign nerve sheath tumor, usually a neurofibroma [2]. NF1 is the most common autosomal dominantly inherited disorder, occurring with a frequency of approximately 1 in 4,000 individuals [3], bringing with it an increased risk of benign and malignant neoplasms. The histogenesis of MPNST remains unclear.

Most aggressive human cancers are characterized by genomic instability [4], which is proposed to be the driving force in the initiation of malignancy such as that seen in colorectal cancer [5]. At least two forms of genomic instability have been described: chromosomal instability (CIN), which is characterized by the loss or gain of chromosomes, and microsatellite instability (MSI), which is characterized by a high frequency of microsatellite instability [6,7]. CIN results from a series of genetic changes that involve the activation of oncogenes such as *KRAS*, and the inactivation of tumor-suppressor genes such as *TP53* and *APC* [8,9]. CIN has been demonstrated in many solid tumors [10]. MSI presents length mutations in microsatellite sequences in

[1] Reprint requests.

* Corresponding author. Tel.: +81-92-642-6067; fax: +81-92-642-5968.

E-mail address: oda@surgpath.med.kyushu-u.ac.jp (Y. Oda).

0165-4608/06/$ – see front matter
doi:10.1016/j.cancergencyto.2005.07.006

oncogenes and tumor-suppressor genes [11,12]. MSI is observed in some hereditary syndromes, such as hereditary nonpolyposis colorectal cancer (HNPCC) [12,13], as well as in sporadic malignancies such as colorectal cancers [14], gastric cancers [15], and endometrial cancers [16]. Recently, an inverse relationship between CIN and MSI has been demonstrated in colorectal cancers; cancers showing mismatch repair (MMR)-deficiency are, in general, diploid and reveal normal rates of gross chromosomal change, whereas MMR-proficient tumors are usually aneuploid and reveal increased rates of chromosomal change [7]. CIN and MSI are suggested to be individual pathways involved in the pathogenesis of colorectal cancer, and may lead to specific clinical and pathological characteristics [17–19].

In MPNST, complex karyotypes with the numerical and structural changes of CIN have been described for nearly all chromosomes [20–27], even though no characteristic cytogenetic alterations were found. Approximately 80 cases of MPNST with variable chromosomal aberrations have been reported to date. To our knowledge, MSI, the other form of genomic instability, has been investigated in only 15 MPNSTs [28,29], and no comprehensive study of the molecular basis behind MSI and CIN has been performed in MPNST.

Therefore, to elucidate the chromosomal aberration as a consequence of CIN and MSI status of MPNST, we karyotyped 10 tumors from nine patients and examined the MSI of seven microsatellite markers using high-resolution fluorescence microsatellite analysis. We also analyzed the relationship between these findings and clinicopathological parameters.

2. Materials and methods

We prepared 10 MPNSTs (9 primary, 1 recurrent) from nine patients (3 male, 6 female) for cytogenetic and microsatellite analysis from the collection of soft tissue tumors registered in the Department of Anatomic Pathology, Pathological Sciences, Graduate School of Medical Sciences, Kyushu University, Japan. The clinicopathological data of the patients are summarized in Table 1.

Age at diagnosis ranged from 1 to 68 years (median: 37 years). There was no previous history of chemotherapy or radiation. Three patients were found to suffer from NF1. Diagnosis in each of the cases was based on histopathological features and immunohistochemical findings, as described by Weiss and Goldblum [2]. Tumor–node–metastasis (TNM) staging was done according to AJCC classification [30].

2.1. Immunohistochemical analysis

Immunostaining for Ki-67 was performed using mouse IgG monoclonal antibodies against Ki-67 (M 7240, 1:100; DakoCytomation, Denmark). After antigen retrieval using a microwave oven technique, the specimens were incubated at 4°C overnight with antibodies to the protein, followed by staining with a streptavidin–biotin–peroxidase kit (Nichirei, Tokyo, Japan) and hematoxylin counterstaining. The Ki-67-labeling index was estimated by counting the number of positive cells per 1,000 tumor cells.

2.2. Cytogenetic analysis

Viable tumor samples were obtained immediately after operation, disaggregated, cultured, harvested, and karyotyped with Giemsa-banding according to standard procedures. Chromosome aberrations and karyotypes were described according to ISCN 1995 [31].

2.3. Microsatellite analysis

Snap-frozen tumor samples and corresponding normal tissues were obtained. For microsatellite analysis, seven dinucleotide microsatellite markers (D2S123, D5S107, D5S346, D10S197, D11S904, D13S175, and D17S250) were selected according to previous reports on MSI detection [32–34]. The primer sequences were as described previously [32]. The 5′ PCR primers were labeled with 6-carboxyfluorescein (6-FAM) or 4,7,2′,4′,5′,7′-hexachloro-6-carboxyfluorescein (HEX). Size markers were labeled with 6-carboxy-X-rhodamine (ROX). DNA derived from the

Table 1
Clinicopathological data for 10 MPNST cases in nine patients

Patient no.	Age, yr	Sex	NF1	Location	Tumor size, cm	Depth	Necrosis	Survival (months)	AJCC stage	Mitosis, cells/10 HPF[a]	Ki-67 index, %
1	1	F		Cauda equina	7	Deep	no	D (86)	III	0	21
1[b]	4	F		Retroperitoneum	6.5	Deep	<50%	D (49)	III	29	38
2	22	M		Right upper arm	9	Deep	<50%	A (52)	III	2	15
3	27	M	+	Left thigh	11	Deep	<50%	D (12)	III	14	27
4	52	F	+	Left chest wall	5	Deep	no	A (68)	IB	0	2
5	61	F		Right thigh	8	Superficial	<50%	A (52)	IIC	1	24
6	68	M		Right lower leg	7	Deep	<50%	A (65)	III	7	31
7	27	F	+	Left lower leg	20	Deep	<50%	A (12)	III	29	40
8	66	F		Right thigh	7	Superficial	no	A (27)	IB	2	15
9	47	F		Left thigh	8	Deep	>50%	A (18)	III	5	15

Abbreviations: A, alive; D, dead; F, female; HPF, high-power field; M, male; MPNST, malignant peripheral nerve sheath tumor.

[a] A high-power field (HPF) measures 0.1734 mm^2.

[b] Recurrence.

tumors was amplified with a 6-FAM-labeled 5′ primer and a cold 3′ primer; DNA from normal tissue was amplified with a HEX-labeled 5′ primer and 3′ primer using a thermocycler (Tgradient, Biometra, Germany). The 50-μL reaction mixture contained 100 mmol/L Tris-HCl, 500 mmol/L KCl, 15 mmol/L $MgCl_2$, 2.5 mmol/L dNTP, 2.5 U Taq DNA polymerase (PerkinElmer, Boston, MA), 2 μmol/L of each primer, and 25 ng of genomic DNA. The thermal conditions were as follows: 1 cycle at 95°C for 5 min; 35 cycles at 95°C for 30 sec, at 55°C for 30 sec, and at 72°C for 30 sec; and 1 cycle at 72°C for 10 min. Then 1 μL of 6-FAM–labeled product, 1 μL of HEX-labeled product, and 0.5 μL of ROX-labeled size marker were mixed with 22.5 μL of tumor-suppressor reagent (Applied Biosystems, Foster City, CA). After denaturization, the mixture was electrophoresed in the same lane using an ABI PRISM 310 sequencer (Applied Biosystems). The data were processed using GeneScan software (Applied Biosystems).

2.4. Evaluation of microsatellite status

Cases showing an additional peak in the tumor DNA compared with their respective normal sample were regarded as being microsatellite unstable for a given marker. Three categories were defined according to the MSI findings; MSI-high (instability at ≥3 microsatellite loci), MSI-low (instability at 1 or 2 loci), and microsatellite stable (MSS; no instability).

2.5. Statistical analysis

Fisher's exact test, chi-square test, Mann–Whitney *U*-test, and McNemar's test were used for statistical analyses. A two-sided *P*-value of <0.05 was considered statistically significant. All tests were performed in consultation with a statistician.

3. Results

3.1. Cytogenetic analysis

Two MPNSTs (20%) had a normal karyotype, while 8 of the 10 MPNSTs (80%) revealed structural and numerical chromosomal aberrations. The clonal changes are listed in Table 2. Frequently involved chromosome bands and commonly detected breakpoints are presented in Fig. 1.

Cases 3, 6, and 7 showed near triploidy. The near-triploidy subgroup showed a significant relation with high Ki-67-labeling index (near-triploidy, median 31%; diploidy, median 15%; $P = 0.0498$, Mann–Whitney *U*-test).

The most frequent aberration was −22 (4 of 10; 40%), followed by +2 (3 of 10; 30%), +14 (30%), −13 (30%), −17 (30%), and −18 (30%). Additionally, **del(1)(p3)**, add(1)(p1), **add(3)(q21)**, +7, **add(7)(p22)**, add(9)(p11), **add(9)(p2)**, +10, add(10)(p11), +11, add(11)(p15), add(12)(q24.1), +13, **add(14)(q32)**, −16, +18, add(19)(p13), −20, −21, **add(21)(p11.2)**, del(22)(q13), add(X)(p11.2), and −Y were observed less commonly (each in 2 of 10 cases; 20%). Several aberrations (here highlighted

Table 2
Karyotypes and microsatellite status of 10 MPNSTs in nine patients

Case no.	Karyotype	Microsatellite status
1a	46,XX[30]	MSS
1b[a]	46,X,add(X)(p11.2),t(5;10)(q13;q24)[15]/46,X,add(X)(p11.2),add(4)(q21),−6,add(8)(q11.2), add(10)(p11.2), add(12)(q24.1),add(12)(q13),−13,add(18)(p11.2),+2mar[15]	MSS
2	40,XY,−3,−4,−5,add(6)(q11.2),+i(8)(q10),−1,add(11)(p15),−14,−17×2,−18,add(19)(p13), −20,−21,−22,+4mar[1]/ 79,idem×2,−15[19]	MSS
3	58,add(X)(q24),−Y,+der(1)add(1)(p11.2)add(1)(q32),+del(1)(p32),+2,+del(3)(p11.2),add(3)(q21), +add(5)(q11.2), +?der(7)add(7)(p22)add(7)(q11.2)×2,+add(8)(p11.2),−9, der(9)add(9)(p24)add(9)(q11), der(11)ins(11;?)(q23;?)t(7;11)(q11.2;q23)×2,add(13)(q21),+14, +14,add(15)(p11.2),add(15)(p11.2), del(16)(p11.2)×2,−17,add(17)(q25),−18,+add(19)(q13.3)×2, add(19)(q13.1),add(21)(p11.2)×2,del(22)(q13),+3mar[20]	MSI-low
4	47,XX,add(8)(q22),del(13)(q32),add(14)(q32),+mar[1]/47,XX,del(1)(p34.1),add(2)(q11.2), der(3)ins(3;?)(p21;?)add(3)(q12),add(12)(q24.1),−13,ins(14;?)(q22;?),add(17)(p11.2),−18, −22,+4mar[1]/ 46,XX[38]	MSS
5	47,XX,+7[2]/46,XX[28]	MSI-low
6	76,−Y,add(X)(p11.2),+add(X)(p22.3),+del(1)(q21),+add(1)(p13),+add(1)(p13),+2,+2, +add(3)(q21)×2, +add(4)(p16)×2,+dup(5)(q31q35)×2,+7,+7,+8,+8,der(9)t(1;9)(p13;p11.2)×2, +add(9)(p11.2)×2,+10,+10,+11, add(12)(p11.2),+add(12)(p11.2),+13,+add(13)(q32),+14, +16,+16,−17,−17,+18,+18,add(19)(p13.1)×2, −20,−20,+6mar[30]	MSS
7	78,X,del(X)(q22),+1,+2,+2,+2,+2,+3,+4,+5,+5,+6,+6,+6,+add(7)(p22)×4,+9,+9, +add(9)(p22),+del(9)(p22)×2, +10,+11,+add(11)(p15),+12,+12,+12,+13,+13,+13,+14, add(14)(q32)×2,−16,+17,+18,+19,add(20)(q13.1)×2, add(21)(p11.2)×2,−22,del(22)(q13)[10]	MSI-low
8	46,XX[20]	MSS
9	44,−X,add(5)(q22),add(8)(p23),add(9)(p11),add(10)(p11),−13,−16,−21,−22,+3mar[20]	MSS

Abbreviations: MSI, microsatellite instability; MSS, microsatellite stable.
[a] Case 1b: recurrence.

in bold) were restricted to NF1-associated patients; however, none of the frequent imbalances were significantly higher in the NF1-associated versus sporadic tumor subgroups. Loss of chromosome 17 was seen only in male patients (P = 0.008, Fisher's exact test). Cases with +2 and +14 were significantly associated with a high Ki-67-labeling index (+2 and +14, median 31%; others, median 15%; P = 0.0498, Mann–Whitney U-test) and tended to have a high mitotic count (+2, 14 per 10 high-power fields; others, 5.6 per 10 high-power fields; P = 0.066, Mann–Whitney U-test).

3.2. Microsatellite analysis

An MSI-low status was observed in three tumors (3 of 10; 30%) (Table 2); of these, case 7 displayed instability at two loci, and cases 3 and 5 exhibited instability at only one locus (Fig. 2). An MSI-low status was significantly associated with a larger tumor size (MSI-low, median 11; MSS, median 7; P = 0.037, Mann–Whitney U-test). No other clinicopathological parameters showed any significant associations with MSI status.

Chromosomal aberration tended to be more frequent than MSI (P = 0.0625, McNemar's test).

4. Discussion

CIN and MSI proved to be two major alternative mechanisms of tumor progression in sporadic colorectal cancers. About 60% of these cancers develop through the CIN pathway [6], tend to be located within the distal colon, and have a stage-independent poor prognosis [35]. In contrast, up to 15% of colorectal cancers show an MSI-high status [33], tend to be distributed within the proximal colon, and demonstrate a favorable outcome [36]. The present study revealed that 8 out of the 10 MPNSTs (80%) displayed complex chromosome structural and numerical rearrangements as a consequence of CIN, whereas 3 out of the 10 tumors (30%) demonstrated only an MSI-low status. None of the tumors had an MSI-high status. Thus, chromosomal aberration tended to be more frequent than MSI.

Because of overlapping, we could not divide our series into two distinct categories; that is, we could not separate out chromosomal aberration-positive and MSI-positive subgroups. It follows from the findings, however, that chromosomal aberration as a consequence of CIN (i.e., large-scale genomic instability) seems to play a greater role in the pathogenesis of MPNST than MSI (i.e., minor-scale genomic instability).

Focusing on the cytogenetic analysis, the results of the present study were in general agreement with previously published data [20–27].

In our series, looking at the two cases (at age 1 and 4 years) for patient 1, chromosomal aberration emerged at the time of recurrence (case 1b) in spite of their absence in the primary state (case 1a). Although our sample size is too small, one explanation for this finding may be that chromosomal aberration is an event that occurs late in tumorigenesis of MPNST. Alternatively, it may be that MPNST has some other mechanism of progression when it occurs in children.

Near triploidy of MPNST, as seen in three of the tumors in the present study, has been reported by several authors as a frequent feature [22,25,27]. Note that triploidy is significantly associated with a high Ki-67-labeling index. Watanabe et al. [37] described a correlation between a high Ki-67-labeling index and poor prognostic features in MPNST. Furthermore, Mertens et al. [27] noted that the presence of triploidy or tetraploidy correlated with poor prognosis.

We found that −22 was the most frequent aberration (40%); loss of 22q was also detected in two tumors (20%). Loss of the chromosomal material of 22q is a relatively frequent event [21,22,25–27]. Comparative genomic hybridization (CGH) studies also showed repeated loss of 22q [38]. Because the genes involved in peripheral and central neurofibromatosis are located in 17q (*NF1*) and 22q (*NF2*), these two regions are of particular interest to MPNST pathogenesis. Nonetheless, no significant difference in the rearrangements between NF-1-associated cases and sporadic cases was recognized in our series.

Loss of chromosome 17 was the second most common alteration (30%); five cases had some abnormality in chromosome 17. The −17 was seen exclusively in male patients (which may be due to bias toward men in NF1 disease). Chromosome 17 is known to contain the tumor-suppressor gene *TP53* in the short arm at 17p13. Large-scale studies have confirmed the frequent loss of both 17p and 17q in MPNST [25–27]. Additionally, a molecular study demonstrated alteration of the *TP53* gene, especially in sporadic cases [39].

Our results also showed frequent loss of chromosome 13 (30%). The *RB* gene is an important tumor-suppressor gene located at 13q14 that regulates the G1–S phase transition of the cell cycle [40]. Mertens et al. [27] reported relatively frequent loss of 13q at the cytogenetic level, and there have been some CGH studies demonstrating imbalances of 13q [38,41,42].

The 9p21 locus, encoding the tumor-suppressor genes *CDKN2A* (for which common aliases include $p16^{INK4A}$ and $p14^{ARF}$), is frequently inactivated in MPNST [42]. This inactivation is considered to be a hallmark of the genetic profile of MPNST [43]. Several alterations were detected in this lesion: add(9)(p11) and add(9)(p2) (each in 2 out of 10 cases, 20%). In all, ≤40% of cases were found to have rearrangement in 9p.

Defective DNA mismatch repair is most commonly associated with the functional loss of *MLH1* and *MSH2* genes, resulting in the mutator phenotype characterized by MSI [44,45]. *MSH2* is located in the 2p21 region, and in the current study, gains of chromosome 2 were observed in 3 of 10 cases (30%). Thus, +2 was present in the high-

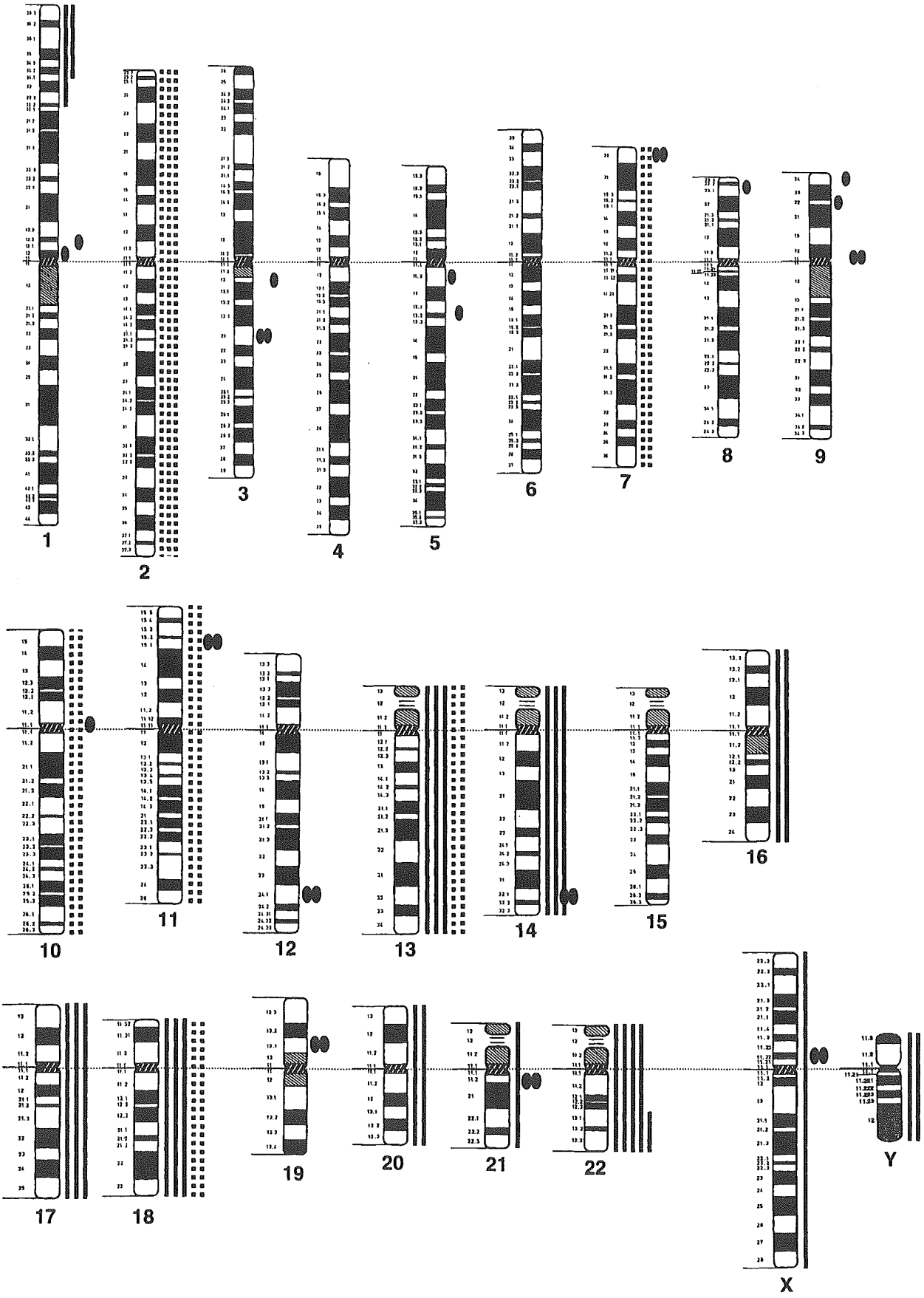

Fig. 1. Summary of the frequent cytogenetic alterations in MPNST. Filled ellipses mark breakpoints. Broken lines indicate chromosomal gain; solid lines indicate loss or deletion.

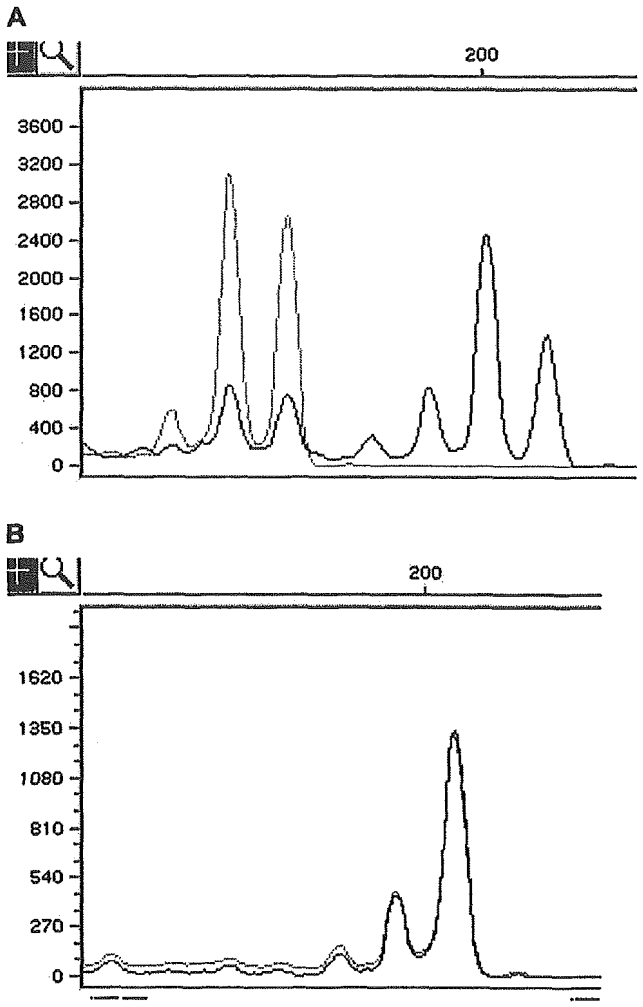

Fig. 2. MSI positivity for the D11S904 microsatellite marker in patient 7 (top panel) and MSS for the same microsatellite marker in Patient 4 (bottom panel). Note difference in vertical scale.

Ki-67- index group, and such cases had a tendency to show high mitotic activity. There is the possibility that numerical aberration involving the *MSH2* gene may result in accelerated tumor proliferation through the mutation of oncogenes or tumor-suppressor genes.

Concerning MSI, there have been several studies describing the presence of MSI in bone and soft tissue sarcomas [28,32,46–50]. Our results show that MSI was present in 3 out of 10 MPNSTs (30%), all of which were tumors with an MSI-low status. These findings are in agreement with previous studies reporting a low frequency of MSI in soft tissue sarcomas [28,46–50]. In the present study, MSI-low status was found to be significantly related with a larger tumor size. Some authors have found an association between MSI and tumor size in cancers [51–53]. If we assume that MSI is an event that occurs late in the progression of MPNST, then we can explain this phenomenon on the grounds that MSI occurs due to increased tumor size.

In conclusion, we analyzed 10 MPNSTs and detected chromosomal aberration in 8 of the tumors (80%) and detected MSI-low status in 3 of them (30%). In general, our findings from the chromosomal and MSI studies were in agreement with those previously reported. This result suggests that chromosomal aberration as a consequence of CIN plays a greater role in the pathogenesis of MPNST, compared with the role played by MSI.

Acknowledgments

This work was supported in part by a Grant-in-Aid for Scientific Research from the Japan Society of the Promotion of Science (15590304), Tokyo, Japan. The English used in this manuscript was revised by Miss K. Miller (Royal English Language Center, Fukuoka, Japan).

References

[1] Ducatman BS, Scheithauer BW, Piepgras DG, Reiman HM, Ilstrup DM. Malignant peripheral nerve sheath tumors: a clinicopathologic study of 120 cases. Cancer 1986;57:2006–21.
[2] Weiss SW, Goldblum JR. Enzinger and Weiss's soft tissue tumors. 4th ed. St. Louis: Mosby, 2001.
[3] Friedman JM. Epidemiology of neurofibromatosis type 1. Am J Med Genet 1999;89:1–6.
[4] Ried T, Heselmeyer-Haddad K, Blegen H, Schrock E, Auer G. Genomic changes defining the genesis, progression, and malignancy potential in solid human tumors: a phenotype/genotype correlation. Genes Chromosomes Cancer 1999;25:195–204.
[5] Stoler DL, Chen N, Basik M, Kahlenberg MS, Rodriguez-Bigas MA, Petrelli NJ, Anderson GR. The onset and extent of genomic instability in sporadic colorectal tumor progression. Proc Natl Acad Sci USA 1999;96:15121–6.
[6] Lengauer C, Kinzler KW, Vogelstein B. Genetic instabilities in human cancers. Nature 1998;396:643–9.
[7] Lengauer C, Kinzler KW, Vogelstein B. Genetic instability in colorectal cancers. Nature 1997;386:623–7.
[8] Vogelstein B, Fearon ER, Hamilton SR, Kern SE, Preisinger AC, Leppert M, Nakamura Y, White R, Smits AM, Bos JL. Genetic alterations during colorectal-tumor development. N Engl J Med 1988;319:525–32.
[9] Fearon ER, Vogelstein B. A genetic model for colorectal tumorigenesis. Cell 1990;61:759–67.
[10] Mitelman F, Johansson B, Mertens F. Catalog of chromosome aberration in cancer. Vol. 2. 5th ed. NewYork: Wiley-Liss, 1994.
[11] Thibodeau SN, Bren G, Schaid D. Microsatellite instability in cancer of the proximal colon. Science 1993;260:816–9.
[12] Ionov Y, Peinado MA, Malkhosyan S, Shibata D, Perucho M. Ubiquitous somatic mutations in simple repeated sequences reveal a new mechanism for colonic carcinogenesis. Nature 1993;363:558–61.
[13] Aaltonen LA, Peltomaki P, Leach FS, Sistonen P, Pylkkanen L, Mecklin JP, Jarvinen H, Powell SM, Jen J, Hamilton SR, et al. Clues to the pathogenesis of familial colorectal cancer. Science 1993;260:812–6.
[14] Lothe RA, Peltomaki P, Meling GI, Aaltonen LA, Nystrom-Lahti M, Pylkkanen L, Heimdal K, Andersen TI, Moller P, Rognum TO, et al. Genomic instability in colorectal cancer: relationship to clinicopathological variables and family history. Cancer Res 1993;53:5849–52.
[15] Wooster R, Cleton-Jansen AM, Collins N, Mangion J, Cornelis RS, Cooper CS, Gusterson BA, Ponder BA, von Deimling A, Wiestler OD, et al. Instability of short tandem repeats (microsatellites) in human cancers. Nat Genet 1994;6:152–6.
[16] Caduff RF, Johnston CM, Svoboda-Newman SM, Poy EL, Merajver SD, Frank TS. Clinical and pathological significance of

microsatellite instability in sporadic endometrial carcinoma. Am J Pathol 1996;148:1671–8.
[17] Gorringe KL, Chin SF, Pharoah P, Staines JM, Oliveira C, Edwards PA, Caldas C. Evidence that both genetic instability and selection contribute to the accumulation of chromosome alterations in cancer. Carcinogenesis 2005;26:923–30.
[18] Kleivi K, Teixeira MR, Eknaes M, Diep CB, Jakobsen KS, Hamelin R, Lothe RA. Genome signatures of colon carcinoma cell lines. Cancer Genet Cytogenet 2004;155:119–31.
[19] Choi SW, Lee KJ, Bae YA, Min KO, Kwon MS, Kim KM, Rhyu MG. Genetic classification of colorectal cancer based on chromosomal loss and microsatellite instability predicts survival. Clin Cancer Res 2002;8:2311–22.
[20] Becher R, Wake N, Gibas Z, Ochi H, Sandberg AA. Chromosome changes in soft tissue sarcomas. J Natl Cancer Inst 1984;72:823–31.
[21] Jhanwar SC, Chen Q, Li FP, Brennan MF, Woodruff JM. Cytogenetic analysis of soft tissue sarcomas: recurrent chromosome abnormalities in malignant peripheral nerve sheath tumors (MPNST). Cancer Genet Cytogenet 1994;78:138–44.
[22] Mertens F, Rydholm A, Bauer HF, Limon J, Nedoszytko B, Szadowska A, Willen H, Heim S, Mitelman F, Mandahl N. Cytogenetic findings in malignant peripheral nerve sheath tumors. Int J Cancer 1995;61:793–8.
[23] McComb EN, McComb RD, DeBoer JM, Neff JR, Bridge JA. Cytogenetic analysis of a malignant triton tumor and a malignant peripheral nerve sheath tumor and a review of the literature. Cancer Genet Cytogenet 1996;91:8–12.
[24] Rao UN, Surti U, Hoffner L, Yaw K. Cytogenetic and histologic correlation of peripheral nerve sheath tumors of soft tissue. Cancer Genet Cytogenet 1996;88:17–25.
[25] Plaat BE, Molenaar WM, Mastik MF, Hoekstra HJ, te Meerman GJ, van den Berg E. Computer-assisted cytogenetic analysis of 51 malignant peripheral-nerve-sheath tumors: sporadic vs. neurofibromatosis-type-1-associated malignant schwannomas. Int J Cancer 1999;83: 171–8.
[26] Fletcher CD, Dal Cin P, de Wever I, Mandahl N, Mertens F, Mitelman F, Rosai J, Rydholm A, Sciot R, Tallini G, van den Berghe H, Vanni R, Willen H. Correlation between clinicopathological features and karyotype in spindle cell sarcomas: a report of 130 cases from the CHAMP study group. Am J Pathol 1999;154:1841–7.
[27] Mertens F, Dal Cin P, de Wever I, Fletcher CD, Mandahl N, Mitelman F, Rosai J, Rydholm A, Sciot R, Tallini G, van den Berghe H, Vanni R, Willen H. Cytogenetic characterization of peripheral nerve sheath tumours: a report of the CHAMP study group. J Pathol 2000;190:31–8.
[28] Kawaguchi K, Oda Y, Takahira T, Saito T, Yamamoto H, Kobayashi C, Tamiya S, Oda S, Iwamoto Y, Tsuneyoshi M. Microsatellite instability and hMLH1 and hMSH2 expression analysis in soft tissue sarcomas. Oncol Rep 2005;13:241–6.
[29] Upadhyaya M, Han S, Consoli C, Majounie E, Horan M, Thomas NS, Potts C, Griffiths S, Ruggieri M, von Deimling A, Cooper DN. Characterization of the somatic mutational spectrum of the neurofibromatosis type 1 (NF1) gene in neurofibromatosis patients with benign and malignant tumors. Hum Mutat 2004;23:134–46.
[30] Sobin LH, Fleming ID. TNM classification of malignant tumors, fifth edition (1997). Union Internationale Contre le Cancer and the American Joint Committee on Cancer. Cancer 1997;80:1803–4.
[31] ISCN 1995: an international system for human cytogenetic nomenclature (1995). In: Mitelman F, editor. Basel: S. Karger, 1995.
[32] Takahira T, Oda Y, Tamiya S, Yamamoto H, Kawaguchi K, Kobayashi C, Oda S, Iwamoto Y, Tsuneyoshi M. Microsatellite instability and p53 mutation associated with tumor progression in dermatofibrosarcoma protuberans. Hum Pathol 2004;35:240–5.
[33] Boland CR, Thibodeau SN, Hamilton SR, Sidransky D, Eshleman JR, Burt RW, Meltzer SJ, Rodriguez-Bigas MA, Fodde R, Ranzani GN, Srivastava S. A National Cancer Institute workshop on microsatellite instability for cancer detection and familial predisposition: development of international criteria for the determination of microsatellite instability in colorectal cancer. Cancer Res 1998;58:5248–57.
[34] Oda S, Maehara Y, Sumiyoshi Y, Sugimachi K. Microsatellite instability in cancer: what problems remain unanswered? Surgery 2002; 131(1 Suppl):S55–62.
[35] Gervaz P, Cerottini JP, Bouzourene H, Hahnloser D, Doan CL, Benhattar J, Chaubert P, Secic M, Gillet M, Carethers JM. Comparison of microsatellite instability and chromosomal instability in predicting survival of patients with T3N0 colorectal cancer. Surgery 2002;131:190–7.
[36] Kim H, Jen J, Vogelstein B, Hamilton SR. Clinical and pathological characteristics of sporadic colorectal carcinomas with DNA replication errors in microsatellite sequences. Am J Pathol 1994;145:148–56.
[37] Watanabe T, Oda Y, Tamiya S, Kinukawa N, Masuda K, Tsuneyoshi M. Malignant peripheral nerve sheath tumours: high Ki67 labelling index is the significant prognostic indicator. Histopathology 2001;39:187–97.
[38] Koga T, Iwasaki H, Ishiguro M, Matsuzaki A, Kikuchi M. Frequent genomic imbalances in chromosomes 17, 19, and 22q in peripheral nerve sheath tumours detected by comparative genomic hybridization analysis. J Pathol 2002;197:98–107.
[39] Birindelli S, Perrone F, Oggionni M, Lavarino C, Pasini B, Vergani B, Ranzani GN, Pierotti MA, Pilotti S. Rb and TP53 pathway alterations in sporadic and NF1-related malignant peripheral nerve sheath tumors. Lab Invest 2001;81:833–44.
[40] Livingston DM, Kaelin W, Chittenden T, Qin X. Structural and functional contributions to the G1 blocking action of the retinoblastoma protein [The 1992 Gordon Hamilton Fairley Memorial Lecture]. Br J Cancer 1993;68:264–8.
[41] Lothe RA, Karhu R, Mandahl N, Mertens F, Saeter G, Heim S, Borresen-Dale AL, Kallioniemi OP. Gain of 17q24-qter detected by comparative genomic hybridization in malignant tumors from patients with von Recklinghausen's neurofibromatosis. Cancer Res 1996;56:4778–81.
[42] Berner JM, Sorlie T, Mertens F, Henriksen J, Saeter G, Mandahl N, Brogger A, Myklebost O, Lothe RA. Chromosome band 9p21 is frequently altered in malignant peripheral nerve sheath tumors: studies of CDKN2A and other genes of the pRB pathway. Genes Chromosomes Cancer 1999;26:151–60.
[43] Perrone F, Tabano S, Colombo F, Dagrada G, Birindelli S, Gronchi A, Colecchia M, Pierotti MA, Pilotti S. p15INK4b, p14ARF, and p16INK4a inactivation in sporadic and neurofibromatosis type 1-related malignant peripheral nerve sheath tumors. Clin Cancer Res 2003;9:4132–8.
[44] Fishel R, Lescoe MK, Rao MR, Copeland NG, Jenkins NA, Garber J, Kane M, Kolodner R. The human mutator gene homolog MSH2 and its association with hereditary nonpolyposis colon cancer. Cell 1993;75:1027–38.
[45] Leach FS, Nicolaides NC, Papadopoulos N, Liu B, Jen J, Parsons R, Peltomaki P, Sistonen P, Aaltonen LA, Nystrom-Lahti M, et al. Mutations of a mutS homolog in hereditary nonpolyposis colorectal cancer. Cell 1993;75:1215–25.
[46] Mastrangelo D, Hadjistilianou T, Mazzotta C, Loré C. Microsatellite instability in three cases of embryonal rhabdomyosarcoma of the orbit. Med Pediatr Oncol 2002;39:132–3.
[47] Aue G, Hedges LK, Schwartz HS, Bridge JA, Neff JR, Butler MG. Clear cell sarcoma or malignant melanoma of soft parts: molecular analysis of microsatellite instability with clinical correlation. Cancer Genet Cytogenet 1998;105:24–8.
[48] Martin SS, Hurt WG, Hedges LK, Butler MG, Schwartz HS. Microsatellite instability in sarcomas. Ann Surg Oncol 1998;5:356–60.
[49] Saito T, Oda Y, Kawaguchi K, Takahira T, Yamamoto H, Sakamoto A, Tamiya S, Iwamoto Y, Tsuneyoshi M. Possible association between tumor-suppressor gene mutations and hMSH2/hMLH1

inactivation in alveolar soft part sarcoma. Hum Pathol 2003;34: 841–9.

[50] Suwa K, Ohmori M, Miki H. Microsatellite alterations in various sarcomas in Japanese patients. J Orthop Sci 1999;4:223–30.

[51] Vaish M, Mishra A, Kaushal M, Mishra SK, Mittal B. Microsatellite instability and its correlation with clinicopathological features in a series of thyroid tumors prevalent in iodine deficient areas. Exp Mol Med 2004;36:122–9.

[52] Gafa R, Maestri I, Matteuzzi M, Santini A, Ferretti S, Cavazzini L, Lanza G. Sporadic colorectal adenocarcinomas with high-frequency microsatellite instability. Cancer 2000;89:2025–37.

[53] Shen KL, Yang LS, Hsieh HF, Chen CJ, Yu JC, Tsai NM, Harn HJ. Microsatellite alterations on human chromosome 11 in in situ and invasive breast cancer: a microdissection microsatellite analysis and correlation with p53, ER (estrogen receptor), and PR (progesterone receptor) protein immunoreactivity. J Surg Oncol 2000;74:100–7.

Histopathology 2005, 47, 357–367. DOI: 10.1111/j.1365-2559.2005.02242.x

Loss of phenotypic expression is related to tumour progression in early gastric differentiated adenocarcinoma

T Nakamura, T Yao, A Kabashima,[1] K Nishiyama, Y Maehara[1] & M Tsuneyoshi
Departments of Anatomic Pathology and [1]Surgery and Science, Graduate School of Medical Sciences, Kyushu University, Fukuoka, Japan

Date of submission 7 April 2004
Accepted for publication 8 November 2004

Nakamura T, Yao T, Kabashima A, Nishiyama K, Maehara Y & Tsuneyoshi M
(2005) *Histopathology* 47, 357–367

Loss of phenotypic expression is related to tumour progression in early gastric differentiated adenocarcinoma

Aims: To evaluate the relationship between phenotypic expression and tumour progression as represented by macroscopic features, submucosal invasion and lymph node metastasis in early differentiated gastric adenocarcinoma.
Methods: One hundred and fifty-five cases of early gastric differentiated adenocarcinoma without any poorly differentiated components were studied. The mucosal and submucosal components of carcinomas and lymph node metastatic lesions were classified into four categories, gastric type (G-type), incomplete intestinal type (I-type), complete intestinal type (C-type) and unclassified type (U-type), based on the combination of the phenotypic expression of HGM (gastric foveolar epithelium), MUC6 (gastric pyloric glands), MUC2 (intestinal goblet cells) and CD10 (small intestinal brush border). In addition, a new classification representing a phenotypic shift from mucosa to submucosa or from primary lesion to lymph node metastasis was established with the categories of preserved group (P-group), loss group (L-group) and acquired group (A-group).
Results: (1) In submucosal carcinoma, U-type was more common in the submucosa (39%) than in the mucosa (9%). (2) U-type was more common in the metastatic lesions (42%) than in the primary lesions (5%). (3) The submucosal component and lymph node metastatic lesions were classified as P-group in 48% and 43% of cases, respectively, and as L-group in 50% and 52% of cases, respectively. (4) Lymph node metastatic lesions comprising undifferentiated carcinoma were classified as L-group in 100% of cases.
Conclusion: During the course of tumour progression, early differentiated adenocarcinoma at first tends to lose its phenotypic expression despite preserving its morphology, but subsequently morphological dedifferentiation occurs.

Keywords: CD10, early differentiated gastric carcinoma, human gastric mucin, MUC2, phenotype

Abbreviation: HGM, human gastric mucin

Introduction

By means of observing standard haematoxylin and eosin (H&E) staining, gastric carcinomas have been divided into two histological types, such as intestinal type and diffuse type by Lauren[1] or differentiated type and undifferentiated type by Nakamura.[2] It is considered that intestinal type carcinoma almost equates to differentiated type carcinoma, and that diffuse-type carcinoma almost equates to gastric or undifferentiated type carcinoma. However, there remain various opinions regarding the classification of gastric carcinoma using mucin-histochemical or immunohistochemical methods. Tatematsu *et al.*[3] and Egashira *et al.*[4] reported that 34.4% and 30.4%, respectively, of differentiated gastric carcinomas showed a gastric phenotype by

Address for correspondence: Takashi Yao, Anatomic Pathology, Faculty of Medicine, Kyushu University, Maidashi 3-1-1, Higashi-ku, Fukuoka 812–8582, Japan.
e-mail: takyao@surgpath.med.kyushu-u.ac.jp
Reprint requests: Masazumi Tsuneyoshi, Anatomic Pathology, Faculty of Medicine, Kyushu University, Maidashi 3-1-1, Higashi-ku, Fukuoka 812–8582, Japan.
e-mail: masazumi@surgpath.med.kyushu-u.ac.jp

immunohistochemical or mucin-histochemical studies. Kabashima *et al.* divided gastric carcinomas into three phenotypes: gastric type, incomplete intestinal type and complete intestinal type, using immunohistochemical methods for human gastric mucin (HGM), MUC2 and CD10.[5] HGM is a marker of gastric foveolar epithelium mucin, whereas MUC2 is a marker of intestinal goblet cell differentiation. CD10 is considered useful for detecting the brush border of the small intestine.[5–7] They also used paradoxical concanavalin A (ConA) as a marker of pyloric glands. Machado *et al.* utilized MUC6 as a marker of gastric mucous neck cells and pyloric glands in place of ConA.[8] It has been reported that gastric phenotype carcinomas tend to favour invasion and metastasis compared with intestinal phenotype carcinomas;[9–15] therefore, phenotypic subclassification could be useful for understanding the biological behaviour of carcinomas and for selecting the appropriate therapy. Egashira *et al.*[4] and Nishikura *et al.*[14] reported that the phenotype of the mucosal layer was apt to be maintained in the submucosa, and that the gastric type did not shift to the intestinal type and the intestinal type did not shift to the gastric type; however, detailed investigations have not been carried out. Furthermore, the phenotypic expression of metastatic lesions has not been reported.

In the current study, we classified the phenotype of early differentiated gastric carcinoma by immunohistochemical methods using the phenotypic expression markers HGM, MUC6, MUC2 and CD10, and we investigated the relationship between phenotype and tumour progression, particularly in (i) elevated and depressed types, (ii) mucosal and submucosal components, and (iii) primary lesions and lymph node metastatic lesions.

Materials and methods

TISSUES STUDIED

From our files of surgically resected gastric specimens at Kyushu University Hospital and its affiliated hospitals, 155 samples of early differentiated gastric adenocarcinoma were selected for the present study. Eighty-five samples comprised elevated type (polypoid or flat elevated type) while 66 samples comprised depressed type (ulcer cases were not included), and the other four samples were of mixed type. Seventy-four samples were intramucosal carcinomas while 81 samples were submucosal carcinomas. We also selected 57 of the 81 submucosal carcinomas, which had invaded deeper than the middle layer of the submucosa (deep submucosa), in order to evaluate further the phenotypic differences between the mucosal and submucosal components. Our discussion of the relationship between mucosal components and submucosal components is based on these 57 samples. Among the submucosal carcinomas, 24 samples were positive for lymph node metastasis (57 lymph nodes) while 57 samples were negative. All the lesions were cut with serial step slices of 3–4 mm in width, fixed in 10% formalin solution and embedded in paraffin.

IMMUNOHISTOCHEMICAL STAINING

Monoclonal antibodies against HGM (45M1; Novocastra, Newcastle, UK) as a marker for gastric foveolar epithelium, MUC6 (CLH5; Novocastra) as a marker for pyloric glands, MUC2 (Ccp58; Novocastra) as a marker for goblet cells and CD10 (56C6; Novocastra) as a marker for the brush border were used. Immunohistochemistry was carried out by the streptavidin–biotin–peroxidase complex method (Histofine SAB-PO Kits; Nichirei Corp., Tokyo, Japan) as described by Kabashima *et al.*[5]

The results of staining were categorized into two groups, positive and negative expression, in accordance with the study by Kabashima *et al.*[5] When > 10% of the carcinoma cells in the neoplastic lesion were stained, the lesion was classified as showing positive expression. When < 10% of the carcinoma cells were stained, the lesion was classified as showing negative expression.

CLASSIFICATION OF PHENOTYPIC EXPRESSION OF CARCINOMAS

The classification of Kabashima *et al.* was used for the phenotyping of the carcinomas[5,7] (Figure 1). The

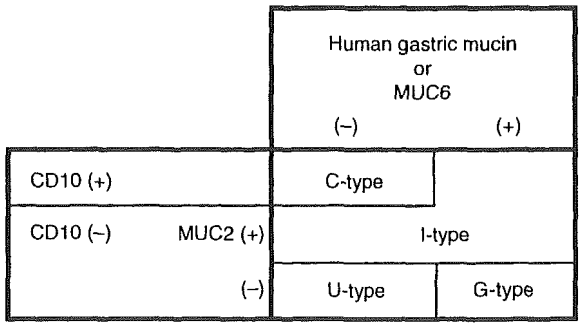

Figure 1. Phenotypic classification: Carcinomas were classified into four categories, gastric type (G-type), incomplete intestinal type (I-type), complete intestinal type (C-type) and unclassified type (U-type), according to the combination of the phenotypic expression of human gastric mucin (HGM), MUC2 and CD10. Exceptionally, G-type also includes pyloric gland type, which is HGM–, MUC2–, CD10– and MUC6+.

phenotypes were classified into four categories according to the combination of the expression of HGM, MUC2 and CD10. Gastric type (G-type) demonstrated positive expression for HGM but negative expression for CD10 and MUC2. Complete intestinal type (C-type) demonstrated positive expression for CD10 but negative expression for HGM, regardless of whether it showed positive or negative expression for MUC2. Incomplete intestinal type (I-type) demonstrated positive expression for both CD10 and HGM, or for both MUC2 and HGM, or else negative expression for these two and positive expression for only MUC2. Unclassified type (U-type) demonstrated negative expression for HGM, MUC2 and CD10. In exceptional cases, when the carcinoma was negative for CD10, MUC2 and HGM, but positive for MUC6, it was classified as G-type (pyloric gland type).

Furthermore, we established three categories to describe the phenotypic shift: (i) preserved group (P-group), (ii) loss group (L-group), and (iii) acquired group (A-group). P-group was defined as those lesions which showed no phenotypic shift, from mucosa to submucosa or from primary lesion to metastatic lesion. L-group was defined as those lesions which showed loss of all or some phenotypic expression (HGM, MUC6, MUC2 or CD10) in the submucosa or metastatic lesions. A-group was defined as those lesions which had some newly acquired phenotypic expression in the submucosa or metastatic lesions.

STATISTICAL ANALYSES

The relationship between phenotype and clinicopathological features, macroscopic features, invasion and lymph node metastasis was examined by the χ^2 test and the Fisher exact probability test. The level of significance was $P < 0.05$.

Results

PHENOTYPE

The typical histological features on H&E sections were as follows (Figure 2). In the case of gastric type (G-type) carcinoma, the carcinoma cells demonstrated clear cytoplasm with relatively uniform round nuclei (Figure 2a). In the case of incomplete intestinal type (I-type) carcinoma, the carcinoma cells demonstrated dark cytoplasm with scattered goblet cells; however, a brush border could not be recognized (Figure 2b). In the case of complete intestinal type (C-type) carcinoma, the carcinoma cells demonstrated dark cytoplasm which resembled small intestinal epithelium (Figure 2c). An example of the immunohistochemical pattern of I-type carcinoma can be seen in Figure 3.

Table 1 shows the relationship between phenotype and clinicopathological features in submucosal carcinomas. Based on the predominant phenotypic expression, the carcinomas were classified into G-type (26%), I-type (54%), C-type (14%) or U-type (6%). However, there were no significant differences between phenotype and clinicopathological features.

Table 2 shows the relationship between phenotype and macroscopic features in early differentiated adenocarcinomas. There were no significant differences in phenotype between the elevated type and the depressed type of lesions.

Table 3 shows the relationship between phenotype and invasion. The phenotypic ratio of the mucosal component was not significantly different between intramucosal and deep submucosal carcinomas. However, in the case of deep submucosal carcinoma, U-type was more common in the submucosa (39%) than in the mucosa (9%).

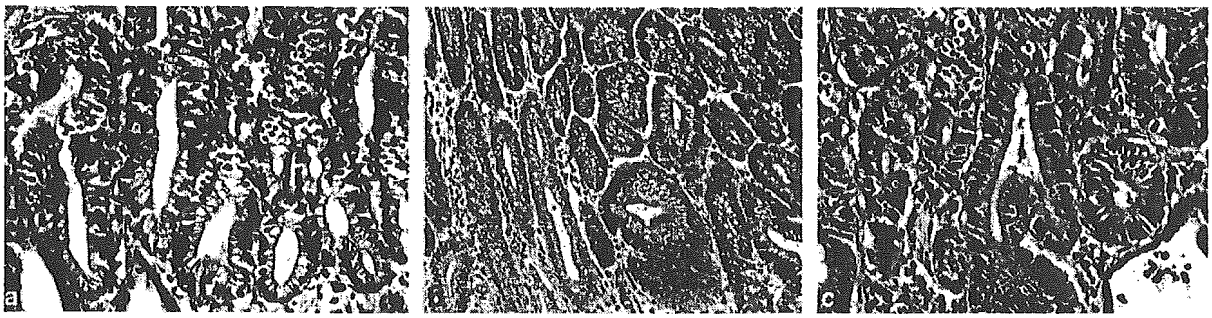

Figure 2. The typical histological features on H&E stain. **a**, Gastric type (G-type) carcinoma. The carcinoma cells have clear cytoplasm with relatively uniform round nuclei. **b**, Incomplete intestinal type (I-type) carcinoma. The carcinoma cells have dark cytoplasm with scattered goblet cells; however, a brush border cannot be seen. **c**, Complete intestinal type (C-type) carcinoma. The carcinoma cells have dark cytoplasm with a brush border, resembling the small intestinal epithelium.

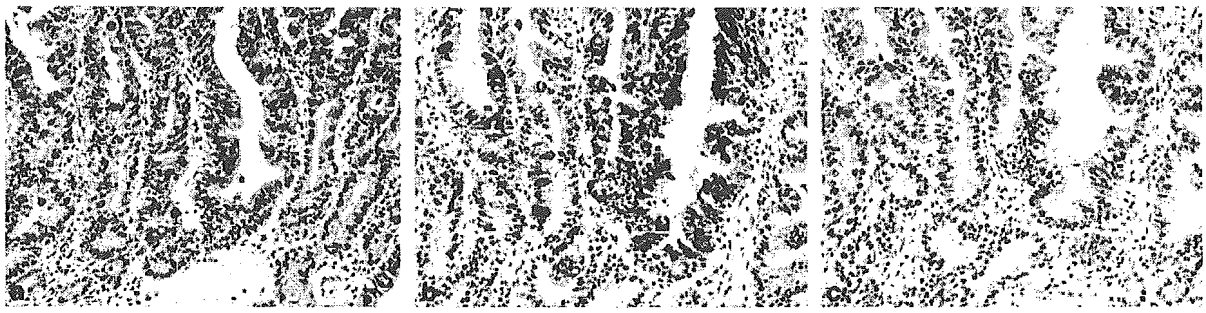

Figure 3. Immunohistochemical expression of I-type carcinoma. **a**, Human gastric mucin is positively expressed in the cytoplasm (45M1). **b**, MUC2 is positively expressed in the goblet cells (Ccp58). **c**, CD10 is not expressed (56C6).

Table 1. Phenotype and clinicopathological features in submucosal carcinoma

Factor	Total	G-type	I-type	C-type	U-type
Case number	81 (100%)	21 (25.9%)	44 (54.3%)	11 (13.6%)	5 (6.2%)
Gender (male : female)	49 : 32	12 : 9	24 : 20	9 : 2	4 : 1
Age, years (mean ± SD)	67.1 ± 10.8	69.3 ± 9.1	66.2 ± 12.3	67.8 ± 8.7	64.0 ± 7.0
Location (U : M : L)*	4 : 48 : 29	1 : 13 : 7	1 : 25 : 18	1 : 7 : 3	1 : 3 : 1
Size, mm (mean ± SD)	38 ± 22	33 ± 22	42 ± 24	32 ± 14	41 ± 15
Positive lymphatic invasion	46 (56.8%)	12 (57.1%)	28 (63.6%)	4 (36.4%)	2 (40.0%)
Positive venous invasion	24 (29.6%)	8 (38.1%)	10 (22.7%)	6 (54.5%)	0 (0%)
Positive lymph node metastasis	24 (29.6%)	7 (33.3%)	15 (34.1%)	1 (9.0%)	1 (20.0%)

G-type, gastric phenotype; I-type, incomplete intestinal phenotype; C-type, complete intestinal phenotype; U-type, unclassified type.
*Upper, middle and lower thirds of the stomach.

Table 2. Phenotype and macroscopic features

Macroscopic feature	G-type	I-type	C-type	U-type
Elevated type (n = 85)	19 (22.4%)	50 (58.8%)	12 (14.1%)	4 (4.7%)
Depressed type (n = 66)	18 (27.3%)	30 (45.5%)	12 (18.2%)	6 (9.1%)

G-type, gastric phenotype; I-type, incomplete intestinal phenotype; C-type, complete intestinal phenotype; U-type, unclassified type.

Table 3. Phenotype and invasion

Depth	G-type	I-type	C-type	U-type
Intramucosal carcinoma (n = 74)	17 (23.0%)	38 (51.4%)	14 (18.9%)	5 (6.8%)
Submucosal carcinoma (n = 57)				
Mucosal component	17 (29.8%)	28 (49.1%)	7 (12.3%)	5 (8.8%)
Submucosal component	14 (24.6%)	13 (22.8%)	8 (14.0%)	22 (38.6%)

G-type, gastric phenotype; I-type, incomplete intestinal phenotype; C-type, complete intestinal phenotype; U-type, unclassified type.

Table 4. Phenotype and lymph node metastasis

Tumour lesion	G-type	I-type	C-type	U-type
Primary lesion ($n = 21$)				
Mucosal component	5 (23.8%)	14 (66.7%)	1 (4.8%)	1 (4.8%)
Submucosal component	4 (19.0%)	8 (38.1%)	1 (4.8%)	8 (38.1%)
Metastatic lesion ($n = 53$)	8 (15.1%)	16 (30.2%)	7 (13.2%)	22 (41.5%)

G-type, gastric phenotype; I-type, incomplete intestinal phenotype; C-type, complete intestinal phenotype; U-type, unclassified type.

Table 4 shows the phenotypic relationship between the primary lesions and the lymph node metastatic lesions. There were 21 cases of deep submucosal carcinoma with lymph node metastasis and the number of metastatic lymph nodes was 53. The ratio of U-type was higher in both the submucosal components (38%) and in the metastatic lesions (42%).

PHENOTYPIC SHIFT (MUCOSA TO SUBMUCOSA)

Figure 4a shows the phenotypic relationship between mucosal and submucosal components in cases of deep submucosal carcinoma. Twenty-nine of the 57 cases had preserved their phenotype (51%) in the submucosa. Eighteen cases had shifted to U-type (32%) while 10 cases had shifted to another phenotype (18%), so in total 28 cases (49%) demonstrated a phenotypic shift from the mucosa to the submucosa. Twenty-six (46%) of these 28 cases had phenotypic shift as a result of loss of all or some phenotypic expression (HGM, MUC6, MUC2 or CD10). In addition, G-type did not shift to C-type, and C-type did not shift to G-type. Table 5a shows the classification of phenotypic shift from mucosa to submucosa in deep submucosal carcinoma. The cases were classified as preserved group (P-group) (51%), loss group (L-group) (46%) and acquired group (A-group) (5%). In all the A-group cases, only CD10 was newly expressed. An example of the phenotypic expression in the mucosa and submucosa can be seen in Figure 5.

Table 6 shows the relationship between phenotypic shift (mucosa to submucosa) and biological behaviour, in particular vessel invasion and lymph node metastasis, but there was no significant difference between the P-group and the L-group.

PHENOTYPIC SHIFT (PRIMARY LESION TO LYMPH NODE METASTATIC LESION)

Figure 4b shows the phenotypic relationship between the primary lesion and the lymph node metastatic lesion. Twenty-five of the 57 metastatic lymph nodes showed a preserved phenotype (44%). Twenty-three cases showed a shift to U-type (40%), while nine cases showed a shift to another phenotype (16%). Twenty-nine (51%) of these 32 cases demonstrated a phenotypic shift to metastasis as a result of a loss of all or some phenotypic expression. Table 5b shows the classification of phenotypic shift from the primary lesion to the metastatic lesion. The cases were classified as P-group (44%), L-group (51%) and A-group (7%). In all the A-group cases, only MUC2 was newly expressed. An example of the phenotypic expression in a lymph node metastatic lesion comprising differentiated carcinoma can been seen in Figure 6.

Table 7 shows further investigation of the relationship between phenotypic shift (primary lesion to lymph node metastatic lesion) and the differentiation of the metastatic lesions. Ten of the 56 lymph node metastatic lesions demonstrated poorly differentiated components, even though the primary lesion demonstrated differentiated carcinoma, and all of these cased were classified as L-group (100%) (Figure 7). On the other hand, the differentiated components of the metastatic lesions were divided into both P-group (52%) and L-group (41%).

Discussion

The relationship between phenotype and clinicopathological or biological features has been investigated in various types of gastric cancer.[5,9–21] However, to date, there has been no detailed discussion with regard to the phenotypic relationship between mucosal and submucosal or primary and lymph node metastatic lesions, in early differentiated gastric carcinomas which do not contain any poorly differentiated components. In this study, we investigated the relationship between phenotype and tumour progression in early gastric carcinomas of differentiated type. In particular, we compared the differences between (i) elevated and depressed types, (ii) mucosal and submucosal components, and (iii) primary and lymph node metastatic lesions.

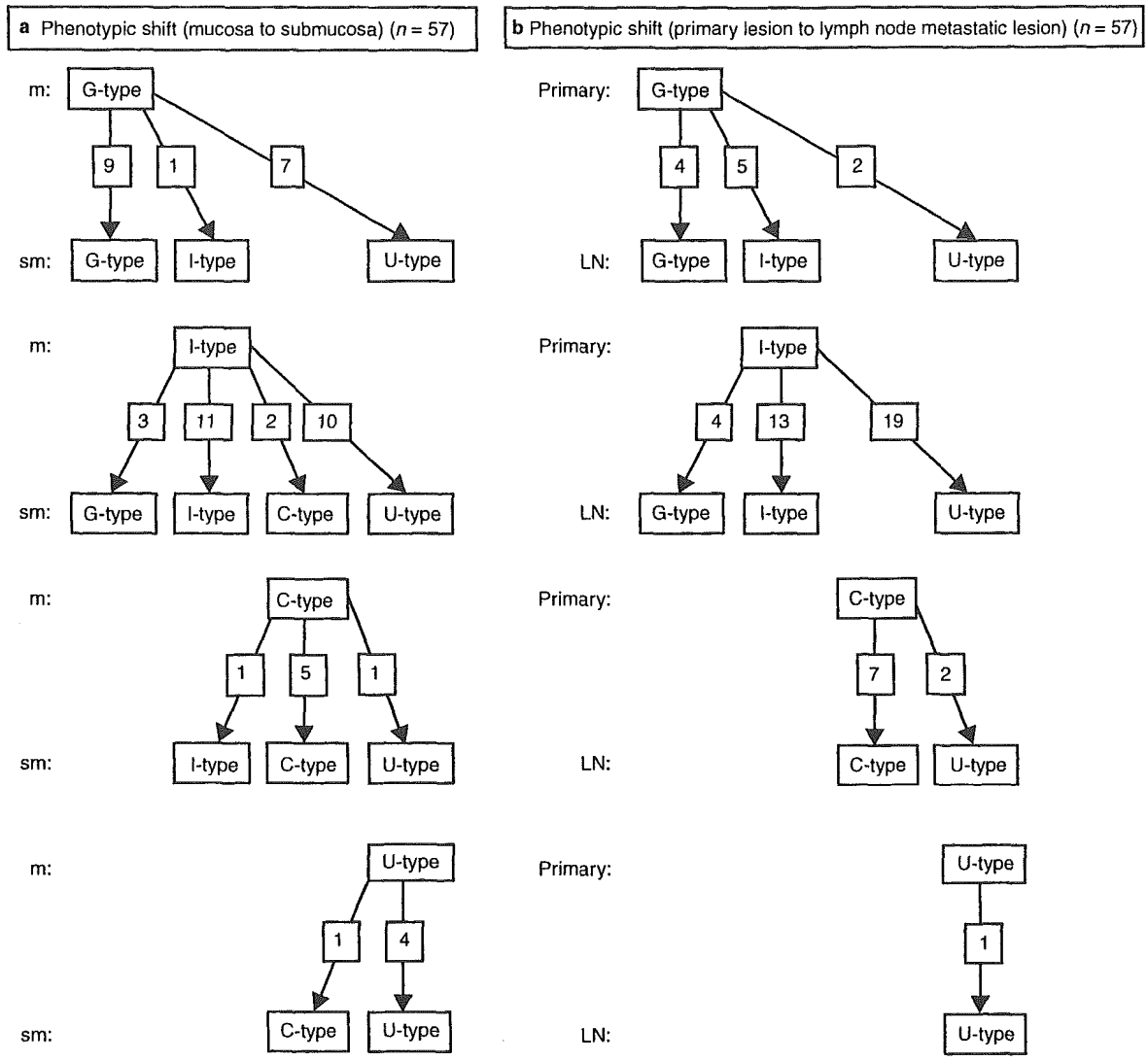

Figure 4. Phenotypic shift. **a,** Relationship between mucosal and submucosal components. The schema shows many cases of phenotypic shift. For example, in a case of incomplete intestinal type (I-type) in the mucosa, which is positive for human gastric mucin (HGM) and MUC2 but negative for CD10, if there is negative shift of MUC2 during the invasion, then the result in the submucosa will be positive for HGM and negative for MUC2 and CD10, and the phenotype in the submucosa will be gastric type (G-type). Such cases were classified as loss group (L-group) because they showed loss of phenotypic expression, namely MUC2 shows a negative shift during the invasion. **b,** Relationship between primary lesions and lymph node metastatic lesions. *m, Mucosal component; sm, submucosal component;* LN, lymph node metastatic lesion.

Phenotypic shift pattern	P-group	L-group	A-group
(a) Invasion (n = 57)			
Mucosa to submucosa	29 (50.9%)	26 (45.6%)* 1	3 (5.2%)* 1
(b) Lymph node metastasis (n = 57)			
Primary lesion to lymph node	25 (43.9%)	29 (50.9%)* 2	4 (7.0%)* 2

P-group, preserved group; L-group, loss group; A-group, acquired group.
*One case showed loss of but also acquired phenotypic expression at the same time.

Table 5. Phenotypic shift from mucosa to submucosa and from primary lesion to lymph node metastasis

Figure 5. Immunohistochemical expression in mucosal and submucosal components. Above the dotted line is the mucosal layer and below is the submucosal layer. **a**, Human gastric mucin is positively expressed in the mucosa, but negatively expressed in the submucosa, so this case shows loss of its phenotypic expression (45M1). **b**, MUC2 is positively expressed in the mucosa, but negatively expressed in the submucosa, so this case shows loss of its phenotypic expression (Ccp58). **c**, CD10 is positively expressed in both the mucosa and the submucosa, so this case shows preservation of its phenotypic expression (56C6).

Table 6. Phenotypic shift (mucosa to submucosa) and biological behaviour (n = 57)

Biological behaviour	P-group (n = 29)	L-group* 1 (n = 26)	A-group* 1 (n = 2)
Lymphatic invasion	16 (55.2%)	15 (57.7%)	2 (66.7%)
Venous invasion	11 (37.9%)	10 (38.5%)	2 (66.7%)
Lymph node metastasis	7 (24.1%)	5 (19.2%)	1 (33.3%)

P-group, preserved group; L-group, loss group; A-group, acquired group.
*One case showed loss of but also acquired phenotypic expression at the same time.

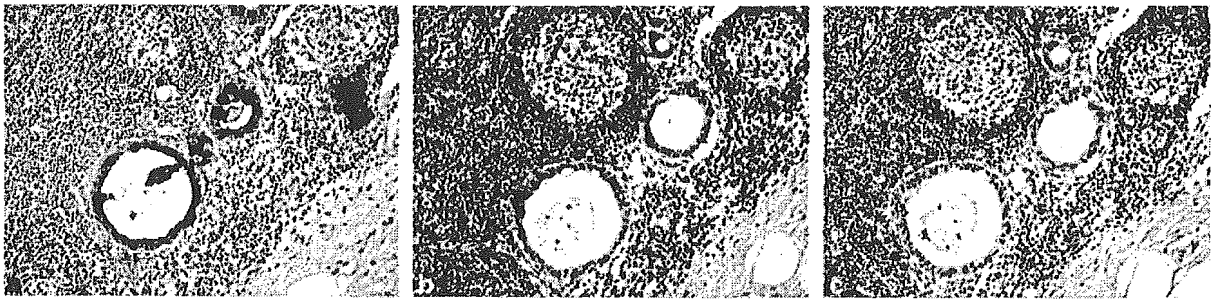

Figure 6. Immunohistochemical expression in a lymph node metastatic lesion comprising differentiated carcinoma. **a**, Human gastric mucin is positively expressed (45M1). **b**, MUC2 is positively expressed (Ccp58). **c**, CD10 is not expressed (56C6).

Table 7. Phenotypic shift (primary lesion to lymph node metastasis) and differentiation of lymph node metastasis

Differentiation	P-group	L-group	A-group
Differentiated (n = 46)	24 (52.2%)	19 (41.3%)*	5 (10.9%)*
Undifferentiated (n = 10)	0 (0%)	10 (100%)	0 (0%)

P-group, preserved group; L-group, loss group; A-group, acquired group.
*Two cases showed loss of but also acquired phenotypic expression at the same time.

Yoshino *et al.*[22] and Oda *et al.*[23] reported that the gastric phenotype macroscopically appears as depressed while the intestinal type appears as elevated. In the current study, however, no relationship was found between phenotype and macroscopic features. The discrepancy of these results may have been due to

